

# Incorporation of montmorillonite in epoxy to obtain a protective layer prepared by electrophoretic deposition

M.F. De Riccardis<sup>a,\*</sup>, V. Martina<sup>a</sup>, D. Carbone<sup>a</sup>, M. Re<sup>a</sup>, E. Pesce<sup>a</sup>, R. Terzi<sup>a</sup>, B. Bozzini<sup>b</sup>

<sup>a</sup> ENEA-Department of Advanced Physical Technologies and New Materials, Brindisi Research Centre, SS 7 Appia, Km 706, Brindisi 72100, Italy

<sup>b</sup> Università del Salento – Dipartimento di Ingegneria dell'Innovazione, via Monteroni, Lecce 73100, Italy

## ARTICLE INFO

### Article history:

Received 14 October 2009

Received in revised form 28 July 2010

Accepted 19 September 2010

### Keywords:

Composite materials

Coatings

Corrosion

Thermal properties

## ABSTRACT

An electrophoretic deposition (EPD) process was successfully used to obtain a composite epoxy coating containing montmorillonite. To disperse and obtain the intercalation of montmorillonite particles, a suitable procedure was optimized. This procedure did not require the use of additional chemicals and it was performed at room temperature.

The microstructural analysis (TEM and XRD) confirmed that the intercalation of montmorillonite layers with epoxy was achieved. Functional characterisations (EIS and TMA) demonstrated the improved properties of the reinforced epoxy coating with respect to the simple epoxy coating.

Moreover, the EPD process resulted more efficient in obtaining a montmorillonite-reinforced epoxy coating than a simple epoxy coating.

© 2010 Elsevier B.V. All rights reserved.

## 1. Introduction

The increased use of metals within all field of technology, included those for special applications such as energy production and saving, imposes to devote more and more attention to metal corrosion, whose costs are considerably elevated in the most highly industrialised countries. A great attention is paid to anti-corrosive paints or coatings, that indeed represent one of the most expensive item among primary corrosion costs.

As protective coatings against corrosion, epoxy represents a class of polymers used frequently, usually placed on steel or metal supports. A low nanoclay loading in epoxy, and in general in polymer materials, can give a positive effect on corrosion resistance, thermo-mechanical properties, and flame retardant characteristics [1–5]. In fact it is expected that the incorporation of nanoclay particles in a polymeric layer could improve its protective properties, thanks to the barrier effect of the layered particles structure, retarding the oxygen and water diffusion toward the coating-metal interface. Usually nanoclay-reinforced polymers are prepared in the form of massive materials by means of traditional methods such as wet casting, open moulding, resin infusion, filament winding, or extrusion. As coatings, ceramic/polymer composites have been principally produced by sol-gel approaches. To the best of the authors' knowledge, there have been no previous publications which have reported protective coatings based on montmorillonite

(MMT) and epoxy resin obtained by electrophoretic deposition (EPD).

EPD is a simple and cheap technique, more frequently used for ceramic casting, that allows also to obtain reliable ceramic coatings [6–8] with an excellent control of thickness and morphology of the deposit through fine-tuning of the deposition parameters. Furthermore, uniform coatings can be obtained on complex shapes and high deposition rates can be achieved, even with low-cost equipment.

With the EPD process, the most critical aspect concerns the starting suspension; a successful EPD requires the achievement of stable suspensions with particles well dispersed in a suitable solvent where appropriate additives prevent particles flocculation or agglomeration. This aspect is particularly critical if the suspension contains more solid components. In spite of its difficult achievement, the preparation of well-dispersed EPD suspension can represent a suitable way to incorporate a reinforcement in a polymer matrix. In fact, by dispersing reinforcement particles, which are in this case nanoclay particles, in a liquid polymer suspension, it is possible to get both a uniform particle distribution in the matrix and some grade of intercalation or exfoliation, that are very attractive achievements in silicate layered reinforced polymers [1,2].

In this work, it is demonstrated the EPD is a suitable method that allows to obtain a composite polymer coating with improved protective properties. These results were achieved by Electrochemical Impedance Spectroscopy measurements (EIS) and thermal analysis. Structural characterisations were performed by TEM and X-ray diffraction.

\* Corresponding author. Tel.: +39 831 201472; fax: +39 831 201540.

E-mail address: [federica.derickardis@enea.it](mailto:federica.derickardis@enea.it) (M.F. De Riccardis).

## 2. Experimental details

An aqueous suspension based on a commercial epoxy resin (Cathoguard 325, BASF, Germany) was prepared by adding 0.1 wt% unmodified nano-MMT (Dellite HPS, Laviosa S.r.l., Italy).

Firstly, 0.1 g of MMT particles was dispersed in 50 ml of water, and then 500 W sonication was applied to the mixture of water and particles. The ultrasound treatment procedure consisted in alternating sonication and rest periods, as detailed below. Particle size measurements were conducted after sonication by NanoSizer ZS (Malvern, GB), in order to evaluate the swelling of the MMT particles. At the same time as the grain size, the zeta potential of the MMT particles suspended in water was evaluated. As expected, no changes in zeta potential accompanied the particle swelling. Then, 47 g of the aqueous suspension of epoxy resin was introduced in the water–MMT particles mixture and further sonication was applied for 10 min. This suspension was used to obtain electrophoretic deposits on plane supports of carbon paper, low carbon steel (A284), and silicon. All sample preparation and deposition procedures were performed at room temperature.

Before epoxy coating deposition, the steel supports were lightly ground with 400 grit SiC paper and phosphatised by immersing in an aqueous solution containing 5 wt%  $H_3PO_4$  and 1.5 wt%  $ZnO_2$  for 20 min at 80 °C, in order to improve the adhesion between epoxy and metal support. Several coated substrates were prepared by EPD; the applied voltage was varied from 5 V to 100 V for MMT–epoxy coating and from 50 V to 350 V for epoxy coating without MMT, to evaluate the deposition rate. After deposition, the resin coatings, both with and without MMT, were cured at 180 °C for 15 min.

To evaluate the deposition rates on different supports, measurements of mass deposited per unit area were performed. When it was necessary, thickness was measured by using a Stylus Profilometer TaylorSurf Intra from Taylor-Hobson.

Coating microstructure and dispersion quality of the MMT particles in epoxy were investigated by transmission electron microscopy (TEM, TECNAI G2 F30) and X-ray diffraction (Wide angle X-ray Diffractometer, RIGAKU Ultima+).

Moreover, the samples were investigated by Electrochemical Impedance Spectroscopy (EIS), yielding information on both the interfacial structure and its effect on the reactivity of the substrate [9]. A potentiostat PAR 2273 in remote control, equipped with a FRA, was used.

Thermo-mechanical analysis (TMA) was carried out in air (TMA 402, NETZSCH). The TMA experiments were performed on resin coatings cured by applying a temperature ramp between 40 °C and 210 °C with a heating rate of 5 °C min<sup>-1</sup>. An hemispherical quartz probe was used to monitor the dimensional changes of the cured resin versus temperature.

## 3. Results and discussion

### 3.1. MMT suspension and deposition process

The layered silicates commonly used for the preparation of polymer/layered silicate nanocomposites belong to the general family of 2:1 layered systems or phyllosilicates. Their crystal structure consists of layers made up of two sheets of tetrahedrally coordinated silicon atoms, fused to an edge-shared octahedral sheet of either aluminium or magnesium hydroxide. The layer thickness is around 1 nm, and the lateral dimensions of these layers may vary from 30 nm to several microns, depending on the particular type of layered silicate. Stacking of the layers leads to a regular van der Waals gap between the layers, called the interlayer or gallery [2].

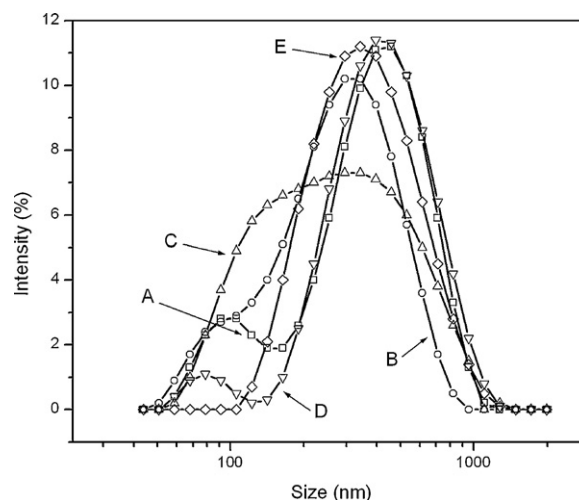


**Fig. 1.** Grain size distribution of the MMT particles measured in different conditions: immediately after mixing (curve A –□–), after 2 h of sonication (curve B –○–), after 2 h of sonication followed by 2 h at rest (curve C –△–), after 4 h of sonication (curve D –▽–), and after 4 h of sonication followed by 4 h at rest (curve E –◇–).

Isomorphic substitution within the layers (for example,  $Al^{3+}$  replaced by  $Mg^{2+}$  or by  $Fe^{2+}$ ) generates negative charges that are counterbalanced by alkali or alkaline earth cations situated in the interlayer. As the forces that hold the stacks together are relatively weak, the intercalation of small molecules between the layers is easy. Montmorillonite, hectorite and saponite – that are the most commonly used layered silicates – are hydrophilic, so both the intercalation within the galleries, initially of water and subsequently of the epoxy aqueous solution, should be relatively easy. For this reason in order to prepare the electrophoretic suspension based on epoxy resin and MMT, the nanoclay particles were initially mixed with water and an appropriate alternation of sonication and rest periods was used, to obtain intercalation of water within the MMT galleries. The introduction of epoxy aqueous solution in the water–MMT suspension, where MMT particles had achieved a swollen condition, enabled the insertion of epoxy resin molecules inside the enlarged galleries of MMT particles. After electrodeposition and curing processes, the epoxy resin molecules were enclosed in MMT silicate layers.

As previously mentioned, the mixture of epoxy and MMT was optimized on the basis of grain size measurements. Following the introduction in water, the MMT grain size shows a bimodal distribution with a lower peak at about 90 nm and an higher one at about 460 nm (see Fig. 1). After sonication for 2 h, the distance between the two peaks of the grain size distribution decreased appreciably, and the lower peak shifted further towards higher grain dimension when a rest period (about 2 h) followed the sonication interval. Then, the water–MMT suspension was sonicated for further 2 h (in total 4 h) and again the grain size showed a bimodal distribution that eventually reached a monomodal distribution after a further rest period of 2 h (4 h overall). For all the measurements, the most intense peak is invariably centred at the same position, close to 400 nm. This behaviour is indicative of a mode of “swelling” of nanoclay particles, related to absorption of mechanical energy from sonication and grain size increase of MMT particles, resulting from the increase of interlayer distance. Measurements of grain size were conducted also after longer time of sonication and rest periods, respectively; the obtained results were essentially the same as those recorded after 4 h of sonication. For this reason, we chose to use MMT–water mixtures treated by sonication for 4 h followed by 4 h at rest, for the preparation of the final bath by addition of the epoxy resin suspension.

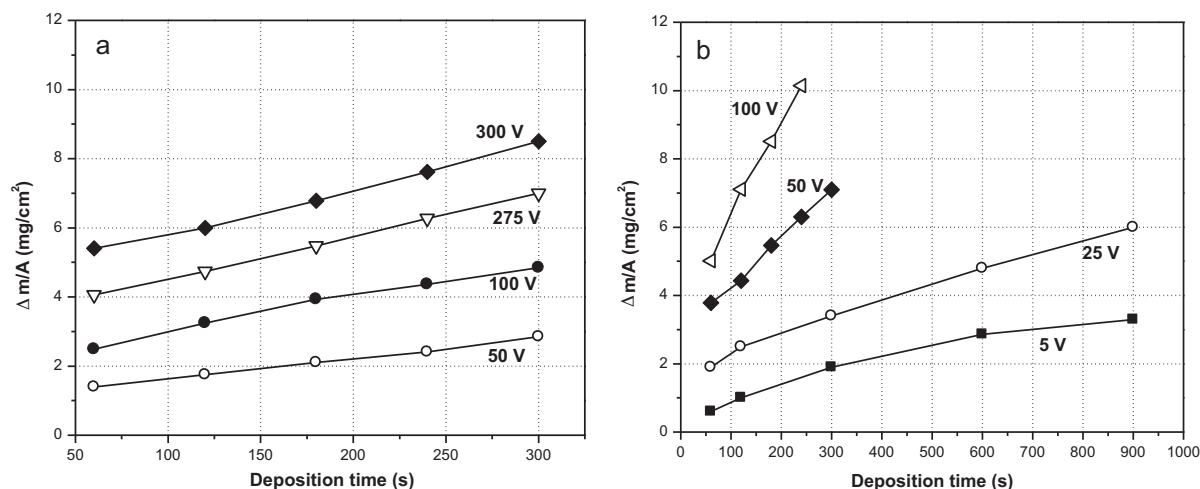


**Fig. 2.** (a) Deposition rates of simple epoxy measured on carbon paper substrates at different applied voltages. (b) Deposition rates of MMT-epoxy measured on carbon paper substrates at different applied voltages.

EPD from the epoxy–MMT suspension was performed by varying the applied potential and the processing time. To evaluate deposition rates at different applied voltages, carbon paper supports were used as working and counter electrodes, because of their easy handling and high conductivity. The gain of deposit mass per unit area is reported in Fig. 2.

Deposition rates measured on carbon paper supports showed that when MMT particles were inserted into the epoxy resin, under otherwise identical deposition conditions, the mass deposited per unit area was higher than without MMT particles. It is noteworthy that an equal value of the deposited mass per area unit was obtained by applying 50 V as voltage to MMT-epoxy suspension and 275 V to simple epoxy suspension. This result is justified by the different conductivity values of the two suspensions:  $1.1 \text{ mS cm}^{-1}$  for the epoxy suspension,  $2.3 \text{ mS cm}^{-1}$  for the MMT-epoxy suspension. One can infer that the addition of MMT particles to the epoxy resin suspension increased the process efficiency. In fact, even if the direct comparison at equal condition is possible only for 50 and 100 V, on the average the deposited mass per area unit measured for epoxy coatings is lower than that measured on MMT-epoxy coatings. In other words, considering the deposited mass per area unit at a fixed time, one can observe that the voltage used to obtain a similar value of the deposited mass is lower in the case of MMT-epoxy coating. From this, we argued that the electrophoretic deposition process is more efficient when MMT is included in the epoxy.

### 3.2. Microstructural characterisation

To observe the epoxy coating by TEM, a thick layer (about  $25 \mu\text{m}$ ) was electrophoretically deposited on a plastic support, suitable for TEM sample preparation, previously gold coated in order to have a conductive surface. From this support a thin slice, about 50 nm thick, was cut by ultramicrotome (TOP-ULTRA 170A, Pabisch) at room temperature. This slice was placed on a Cu grid. TEM observations were performed at 300 kV at low-dose, in order to avoid electron-beam damaging of the sample.

In Fig. 3 a Bright Field TEM image of the epoxy–MMT coating at low magnification is shown; MMT particles are homogeneously distributed inside the coating layer. The Bright Field image reported in Fig. 4 at higher magnification, shows that most of the layers of MMT, relative to (001) planes, are intercalated with the epoxy resin, and in some part they are also exfoliated, resulting in an increased interplanar distance. The distance between two layers, evaluated in many images of several areas, ranged from 2.5 nm to 6.2 nm, wider than that of pristine MMT (1.2 nm).

A typical EDS spectrum of one of these features – acquired in the spot mode – is reported in Fig. 5 and shows the characteristic X-ray peaks of Si, Al, O, and Mg (Cu peaks are due to support grid), confirming that the observed structure is indeed MMT.

As a complementary technique to TEM, XRD is commonly used to identify intercalated structures. It is well known that in such composites containing an intercalated layered silicate, the repetitive multilayer structure is well preserved, allowing the interlayer spacing to be determined. The intercalation of the polymer chains usually increases the interlayer spacing, in comparison with the spacing of the pristine clay, leading to a shift of the diffraction peak towards lower angle values (angle and layer spacing values being related through the Bragg's relation). XRD measurements performed on epoxy–MMT coating (see Fig. 6) revealed a broad diffraction peak centred at about  $\theta = 6^\circ$ , shifted at lower diffraction angles in comparison to the characteristic MMT peak recorded at  $\theta = 7^\circ$ . This shift indicates an higher interlayer spacing of MMT incorporated into the epoxy coating, and confirms the successful intercalation of MMT layers assessed by TEM (see Fig. 4).

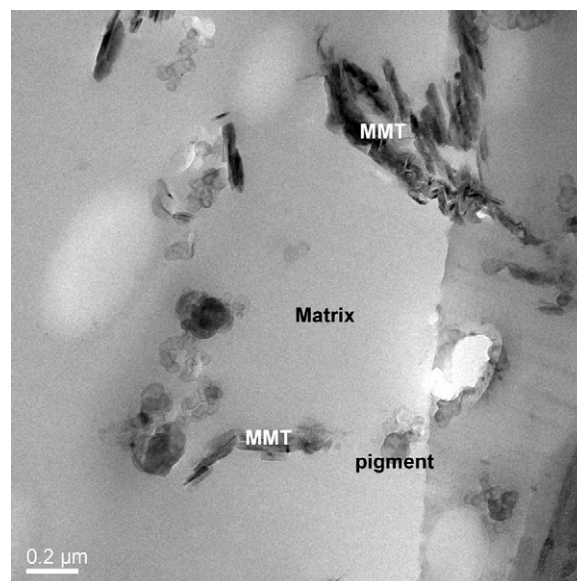


**Fig. 3.** A Bright Field TEM image at low magnification of MMT-epoxy coating.



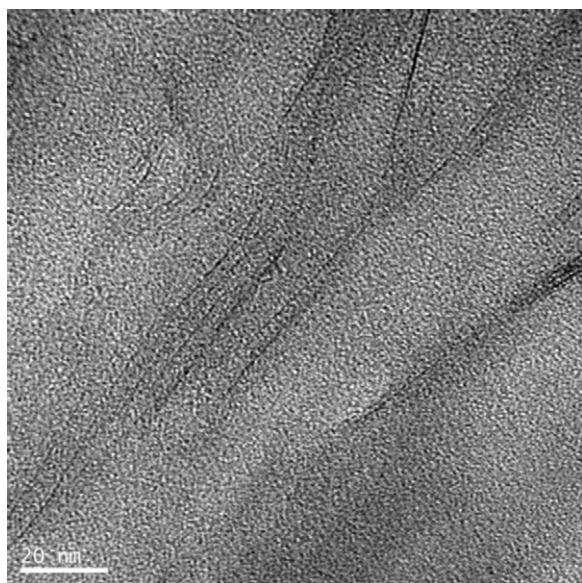


**Fig. 4.** A Bright Field TEM image at high magnification, showing the successful intercalation of MMT layers with epoxy.

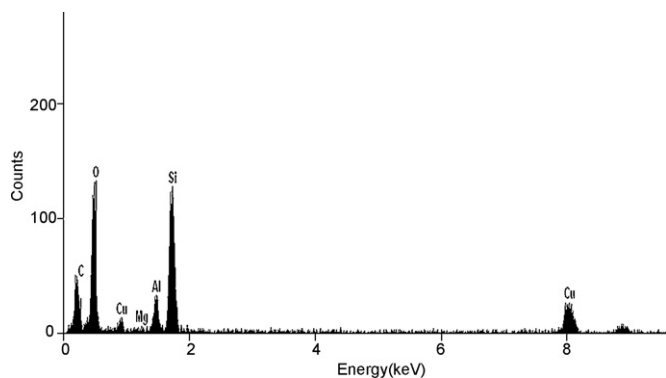


**Fig. 5.** EDS spectrum acquired with the electron beam focused on the MMT particles.

### 3.3. Functional characterisation

The purpose of the incorporation of MMT in an epoxy layer is typically to enhance the anticorrosion properties of the simple

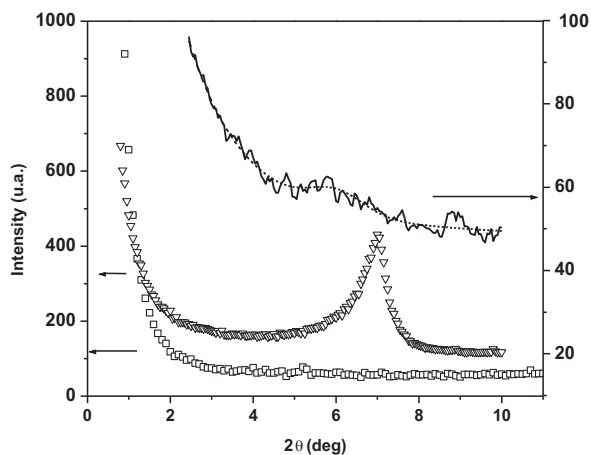


**Fig. 6.** XRD spectra of simple epoxy (open squares) and MMT-epoxy coatings (solid line), as well as of MMT powder (open triangle). A dashed line was added to the signal from MMT-epoxy coating for an easier visualization of the broad diffraction peak at 6°.

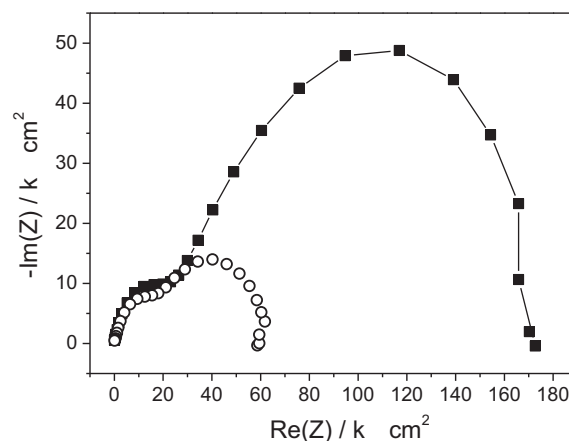


**Fig. 7.** Typical Nyquist impedance diagrams of simple resin-coated steel. Deposition time: 5 min, bias = 0 mV (squares), bias = 75 mV (open circles) as indicated.  $V_{pp} = 10$  mV, frequency range: 100 kHz–5 MHz.

epoxy coating. Electrochemical Impedance Spectroscopy (EIS) is a widely used electrochemical method specially suited for the characterisation of protective organic coating applied on metals. To this aim, epoxy and MMT-epoxy coatings were deposited by EPD on low carbon steel substrates. To coat A284 substrates, the used deposition parameters were those which allowed to obtain approximately the same values of the deposited mass per area unit for the different suspensions, namely 50 V for MMT-epoxy and 275 V for simple epoxy. We investigated two different epoxy and MMT-epoxy coatings, obtained with deposition times of 5 and 10 min, representative of typical industrial coatings. Even if the measured samples had the same deposited mass per area unit, possible differences in thickness between simple epoxy and composite layers, due to the presence of a secondary lighter phase in the epoxy, were negligible since its volume fraction is low.

EIS measurements were conducted in NaCl  $0.35 \text{ g L}^{-1}$ , using a three-electrode configuration with biases corresponding to overvoltages of 0 and 75 mV. The former overvoltage corresponds to the corrosion potential and the latter to free-corrosion of the steel substrate. In this work we chose to carry out EIS measurements under free-corrosion conditions, in order to achieve more detailed information regarding the corrosion performance of the investigated coatings. We restricted this investigation to just one overvoltage because for the studied steel the corrosion mechanism would not change in correspondence of other polarisations. The choice of 75 mV is dictated by two main concerns: (i) lower overvoltages would be too close to the linear Butler-Volmer branch and (ii) more anodic conditions would yield excessive non-stationarities, impacting the statistical reliability of the measured impedance spectra [9–11]. The sine wave amplitude was  $10 \text{ mV}_{pp}$  and the frequency range 100 kHz–5 MHz. The reference electrode was Ag/AgCl and the counter electrode was a Pt wire. The reference electrode was brought into contact with the working electrolyte through a special hydraulic connection, ensuring that no  $\text{Cl}^-$  contamination occurred [12]. A selection of typical Nyquist plots is shown in Fig. 7. The other impedance loci exhibit essentially the same topology, but with notable changes in the values of the real and imaginary parts of the impedance – not reported here for clarity. The Bode plots of the respective moduli of all measurements are displayed in Fig. 8, reporting the impedance moduli for resin coatings without (symbols) and with (lines) added MMT, at bias overvoltages 0 mV (Fig. 8a) and 75 mV (Fig. 8b). The impedance diagrams obtained both in the absence and in the presence of MMT, exhibited the typical behaviour of an active corrosion through a porous protective layer. The lower-frequency RC loop was fitted with a depressed-

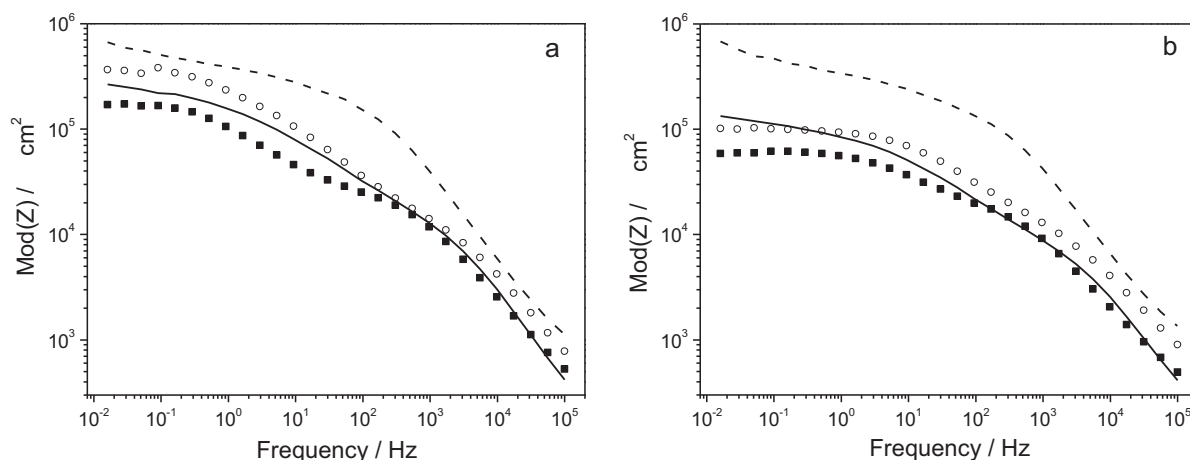


**Fig. 8.** (a) Bode plot of the impedance modulus for resin coatings without (symbols) and with (lines) added MMT. Bias: 0 mV vs. Ag/AgCl. Deposition times: 5 min squares and solid line; 10 min open circles and dashed. (b) Bode plot of the impedance modulus for resin coatings without (symbols) and with (lines) added MMT. Bias: 75 mV vs. Ag/AgCl. Deposition times: 5 min squares and solid line; 10 min open circles and dashed.

circle model, yielding two parameters, diagnostic of the coating quality: (i) the pore resistance  $R_p$  – positively correlated with the impermeability of the coating to water and (ii) the depression angle  $\theta$ , positively correlated with mesoscopic surface roughness. For details on the relevant EIS models, see e.g. [13].

$R_p$  and  $\theta$  values obtained by NLLS of the equivalent-circuit model proposed in [9] are listed in Tables 1a and 1b. The resin without MMT exhibited a protective action that correlates positively with the deposition time, as it can be assessed from the increasing values of  $\text{Mod}(Z)$  and  $R_p$  (Tables 1a and 1b). Corrosion resistance was enhanced by the addition of MMT, both at the corrosion potential (0 mV) and under free-corrosion conditions (75 mV). The effects of time of deposition, and therefore of thickness, on corrosion performance at the corrosion potential (0 mV) were much less marked in the presence of MMT and high corrosion resistance was achieved even with the thinner coating investigated. To the contrary, thicker MMT-containing coatings were found to impart a notable enhancement in corrosion resistance under free-corrosion conditions (75 mV). This difference can be understood in terms of the differences in corrosion mechanism, corresponding to the two electrochemical conditions. At open-circuit the coupling of the substrate to the electrolyte is more critical, since the corrosion rate is controlled by environmentally available oxidants; in this sense, the mass-transport properties of coatings are little affected by the thickness and therefore this variable has a limited effect on corrosion resistance. To the contrary, under free-corrosion conditions, the oxidising action is provided by the applied electrochemical polarisation and the ability of the coatings to fix corrosion products – perhaps in the MMT galleries – can bring about an improvement of the corrosion resistance. Of course, a more insightful structural and chemical investigation of the coatings during the corrosion process – beyond the scope of the present paper – would be needed in order to fully assess the corrosion protection mechanism afforded by the incorporation of MMT into the epoxy layers.

As far as depression angle values are concerned, invariably lower  $\theta$  values were found for the coatings without MMT, denoting lower capacitance dispersion. This quantity was proved to correlate positively with average geometrical roughness [13]. In the case of epoxy without added MMT,  $\theta$  tended to increase when an anodic bias of 75 mV was applied. To the contrary, this parameter was not affected by anodic polarization in the presence of MMT. This behaviour can be interpreted in terms of improved corrosion resistance of MMT-epoxy layer, coherently with the trend found in the analysis of the parameter  $R_p$ .

In order to gain a more insightful understanding of the  $\theta$  estimates, we evaluated the root-mean square roughness  $R_q$  and the surface texture parameter  $R_{Sm}$  [14] by using a TaylorSurf Intra Profilometer.  $R_{Sm}$  values were estimated from profiles acquired along several directions in the deposit plane. The corresponding results are also reported in Tables 1a and 1b.  $\theta$  and  $R_q$  were found to correlate well, confirming that the composite layers were notably rougher, owing to the presence of micrometric MMT platelets. Significantly lower  $R_{Sm}$  values were measured with MMT-containing samples, denoting a lower degree of lateral correlation of the composites, as conformed by optical microscopy observations, not reported for brevity.

The addition of MMT was thus shown to increase the corrosion resistance of epoxy coatings. Higher  $R_p$  values were measured as well as a lower sensitivity to degradation under applied anodic polarization. Furthermore, electrochemical roughness estimates witnessed an enhanced geometrical stability of the composite layers.

In order to evaluate the effect of the addition of MMT particles on the thermal behaviour of epoxy coatings, TMA measurements were performed on simple epoxy and MMT-epoxy coatings. Silicon substrates were used in order to minimise measurement uncertainties related to sample roughness. A plot of  $\Delta L/L_0$  measured on simple epoxy and MMT-epoxy coatings, as a function of the temperature in the range between 40 °C and 210 °C, is reported in Fig. 9. The initial coating thickness  $L_0$  was measured at 25 °C. An appropriate cor-

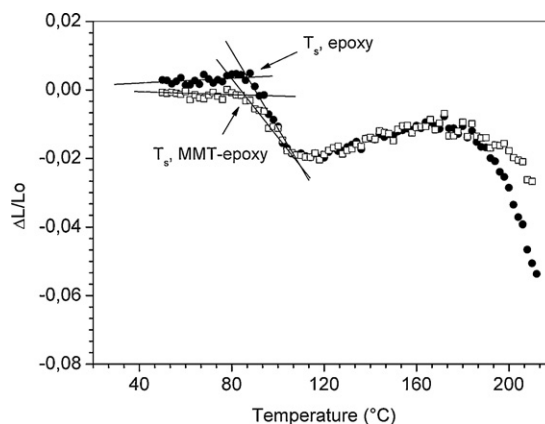


**Fig. 9.** Relative expansion  $\Delta L/L_0$  of simple (closed circle) and reinforced epoxy (open square) coatings.

**Table 1a**

Pore resistance  $R_p$ , depression angle  $\theta$ , root-mean square roughness  $R_q$  and surface texture parameter  $R_{sm}$  values of epoxy coatings without MMT. 95% confidence intervals for  $R_p$  and  $\theta$  as well as standard deviations for  $R_q$  and  $R_{sm}$  are reported.

Deposition time (min)	RP (k $\Omega$ cm <sup>2</sup> )		$\theta$ (deg)		$R_q$ ( $\mu$ m)	$R_{sm}$ ( $\mu$ m)
	Overvoltage 0 mV	Overvoltage 75 mV	Overvoltage 0 mV	Overvoltage 75 mV		
5	146.30 $\pm$ 0.09	48.37 $\pm$ 1.53	12.99 $\pm$ 6.35	29.52 $\pm$ 28.54	0.73 $\pm$ 0.18	219 $\pm$ 86
10	344.70 $\pm$ 5.58	94.36 $\pm$ 0.37	14.97 $\pm$ 8.21	16.06 $\pm$ 7.14	0.58 $\pm$ 0.26	185 $\pm$ 115

**Table 1b**

Pore resistance  $R_p$ , depression angle  $\theta$ , root-mean square roughness  $R_q$  and surface texture parameter  $R_{sm}$  values of epoxy coatings with MMT. 95% confidence intervals for  $R_p$  and  $\theta$  as well as standard deviations for  $R_q$  and  $R_{sm}$  are reported.

Deposition time (min)	RP (k $\Omega$ cm <sup>2</sup> )		$\theta$ (deg)		$R_q$ ( $\mu$ m)	$R_{sm}$ ( $\mu$ m)
	Overvoltage 0 mV	Overvoltage 75 mV	Overvoltage 0 mV	Overvoltage 75 mV		
5	563.01 $\pm$ 22.88	334.93 $\pm$ 22.75	57.94 $\pm$ 3.30	59.95 $\pm$ 5.28	5.72 $\pm$ 0.85	82 $\pm$ 18
10	539.26 $\pm$ 47.33	712.51 $\pm$ 80.26	39.59 $\pm$ 10.95	51.46 $\pm$ 11.34	4.53 $\pm$ 0.70	91 $\pm$ 35

rection procedure was used to eliminate the effect of the substrate thermal expansion.

Both curves showed a first linear shrinkage at roughly 85 °C, corresponding to the softening temperature  $T_s$  of the cured resin. At  $T_s$  the test specimen softened and the probe showed a downward deflection. The curves related to simple and reinforced material did not show any significant difference in the softening temperature. At higher temperatures both curves showed a second shrinkage due to thermal degradation and consequent decomposition of the coating. It is worth noting that the degradation of the MMT–epoxy coating occurred at a lower rate than that of the simple epoxy coating. This behaviour is due to the MMT particles presence in the epoxy coating.

#### 4. Conclusions

Nanoclay particles were successfully incorporated in an aqueous solution of a commercial epoxy resin. This suspension was used to obtain a thin layer on conductive supports, such as carbon paper, low carbon steel, and silicon, by the electrophoretic deposition process. The obtained coatings were tested from the functional point of view, so electrochemical and thermo-mechanical investigations were performed on the nanocomposite polymer coatings in order to evaluate their anticorrosion and thermal performances. The chief results are summarised below.

- (1) The intercalation of unmodified MMT particles was obtained in a straightforward way by alternating sonication and rest intervals at room temperature, without adding any extraneous chemical.
- (2) EIS measurements demonstrated nanocomposite-MMT coatings exhibit higher corrosion resistance than simple epoxy layers, yielding optimal corrosion resistance.
- (3) The thermal degradation of the MMT–epoxy coatings occurs at a lower rate than that of simple epoxy films.

Moreover, by comparing the results obtained both in absence and in presence of MMT particles in the epoxy suspension, we could conclude that the electrophoretic deposition is able to produce coatings with comparable values of the deposited mass per area unit at lower applied voltage when MMT was added to epoxy.

The combination of all these results, suggests a notable industrial potential in the field of corrosion protection can be attributed to the electrophoretic deposition process, that, if applied to nanoclay-reinforced thermosetting polymers, seems to allow the preparation of protective coatings with better performances at lower costs.

#### Acknowledgment

The authors would like to thank E. Calò for XRD measurements.

#### References

- [1] D.R. Paul, L.M. Robeson, *Polymer* 49 (2008) 3187.
- [2] M. Alexandre, P. Dubois, *Mater. Sci. Eng. R* 28 (2000) 1.
- [3] A. Dasari, R.D.K. Misra, J. Rohrmann, *Polym. Eng. Sci.* 44 (2004) 1738.
- [4] J.M. Yeh, C.L. Chen, Y.C. Chen, C.Y. Ma, K.R. Lee, Y. Wei, S. Li, *Polymer* 43 (2002) 2729.
- [5] C.K. Lam, H.Y. Cheung, K.T. Lau, L.M. Zhou, M.W. Ho, D. Hui, *Composites B* 36 (2005) 263.
- [6] A.R. Boccaccini, C. Kaya, K.K. Chawa, *Composites A* 32 (2001) 997.
- [7] O. Van der Biest, L.J. Vandeperre, *Ann. Rev. Mater. Sci.* 29 (1999) 327.
- [8] A.R. Boccaccini, I. Zhitomirsky, *Curr. Opt. Solid State Mater. Sci.* 6 (2002) 251.
- [9] B. Bozzini, I. Sgura, *Nonlinear Anal.: Real World Appl.* 9 (2008) 412.
- [10] B. Bozzini, G.P. De Gaudenzi, C. Mele, *Corros. Eng. Sci. Technol.* 40 (2005) 290.
- [11] I. Sgura, B. Bozzini, *Int. J. Non-Linear Mech.* 40 (2005) 557.
- [12] B. Bozzini, L. D'Urzo, C. Mele, B. Busson, C. Humbert, A. Tadjeddine, *J. Phys. Chem. C* 112 (2008) 11791.
- [13] D.D. Macdonald, in: R. Sarma, J.R. Selman (Eds.), *Techniques for Characterization of Electrodes and Electrochemical Processes*, John Wiley & Sons, Inc., New York, 1991, p. 551.
- [14] P.J. Scott, *Meas. Sci. Technol.* 17 (2006) 559.